Memorias de SICEL 2023 | UNIVERSIDAD NACIONAL DE COLOMBIA

Emulation platform of a Synchronous Machine Wind Generator for an experimental microgrid environment

Plataforma de emulación de un Aerogenerador de máquina síncrona para un entorno experimental de microrred eléctrica

Julian Ontibon-Velasquez[1], Nelson Diaz-Aldana[2], Javier Guacaneme-Moreno[3]

[1] Alternative Energy Sources Research Laboratory (LIFAE), Faculty of Engineering, Universidad Francisco Jose de Caldas, Colombia. Orcid: 0009-0008-6909-4670. Email: jdontibonv@udistrital.edu.co
[2] Alternative Energy Sources Research Laboratory (LIFAE), Faculty of Engineering, Universidad Francisco Jose de Caldas, Colombia. Orcid: 0000-0003-0202-0489. Email: nldiaza@udistrital.edu.co
[3] Alternative Energy Sources Research Laboratory (LIFAE), Faculty of Engineering, Universidad Francisco Jose de Caldas, Colombia. Orcid: 0000-0002-5480-8588. Email: jguacaneme@udistrital.edu.co

Recibido: 22/06/2023. Aceptado: 22/08/2023. Versión final: 07/09/2023

Abstract

Emulation and experimental validation of electrical systems is key to understanding their dynamics and developing various control techniques. This article describes the creation of a prototype using Opal RT platforms, and the LD Didactic electric machine control system, connected via fiber optic. Signals are transmitted using pulse width modulation (PWM) to achieve complete isolation between devices and obtain information on mechanical variables of torque and speed in both control centers. The objective is to emulate a prototype of wind generation in a microgrid and review the power flow supplied by a synchronous machine. This machine is imposed a fixed speed, which allows the power converter to be synchronized and power to be extracted. This gives rise to the development of a dynamic platform that simulates various conditions of a wind generation system.

Keywords: Coupling, Electric machine, Microgrid, Power, Speed, Torque.

Resumen

La emulación y validación experimental de sistemas eléctricos es clave para comprender sus dinámicas y desarrollar diversas técnicas de control. En este artículo se describe la creación de un prototipo utilizando las plataformas Opal RT y el sistema de control de máquinas eléctricas de LD Didactic, conectadas a través de fibra óptica. Las señales se transmiten mediante ancho de pulso (PWM) para lograr un completo aislamiento entre los dispositivos y obtener

How to cite: J. Ontibon-Velasquez, N. Diaz-Aldana and J. Guacaneme-Moreno, "Emulation platform of a Synchronous Machine Wind Generator for an experimental microgrid environment" in *XI Simposio Internacional de Calidad de la Energía Eléctrica*, Valledupar: Universidad Nacional de Colombia, Nov. 2023. doi: https://doi.org/10.15446/sicel.v11.109291

información sobre variables mecánicas de par y velocidad en ambos centros de control. El objetivo es emular un prototipo de generación eólica en una microrred y revisar el flujo de potencia suministrado por una máquina síncrona. A esta máquina se le impone una velocidad fija, lo que permite sincronizar el convertidor de potencia y realizar la extracción de potencia. Esto da lugar al desarrollo de una plataforma dinámica que simula diversas condiciones de un sistema de generación eólica.

Palabras clave: Acoplamiento, Maquina eléctrica, Microrred, Par, Potencia, Velocidad.

1. Introduction

In Colombia, different types of electricity generation are being developed, including cogeneration, photovoltaic energy, wind energy, small hydroelectric power plants, biomass, and geothermal energy [1]. Currently, the country's energy generation is mainly distributed between hydraulic and thermal sources, with a small proportion coming from cogenerators, solar energy, and wind energy [2]. However, it is projected that by 2050, solar and wind energy generation will become the main source, while hydraulic energy will decrease and thermal energy will represent a smaller proportion [2]. The demand for electricity in Colombia is expected to continue increasing in the coming years, which necessitates the development of electric microgrids for efficient management of renewable resources [3] [4].

Studies in the field of microgrids have taken a variety of perspectives. [5] Provides a review of the microgrid concept, its types and control strategies, highlighting challenges and future directions. [6] Explores the use of microgrids in military contexts, highlighting their reliability and flexibility. In addition, [7] analyzes how blockchain technology can improve microgrid cybersecurity by providing a decentralized transaction ledger. [8] Highlights the usefulness of energy management systems (EMS) for optimizing the efficiency of microgrids. [9] Demonstrates the implementation of an EMS in a residential microgrid, managing the flow of energy. [10] Provides a comprehensive overview of technical and economic aspects of microgrids, identifying key research areas. Finally, [11] underscores the importance of energy management and control systems (EMCS) for reliable operation of microgrids. Together, these works offer a complete understanding of the evolution and applications of microgrids.

In this field of work, it is necessary to have laboratories where emulations of different types of energy generation are developed. For this purpose, different electrical devices must be used to manipulate different variables on the overall system. This article focuses on the development of an experimental platform for wind turbine emulation using a synchronous machine to emulate direct conditions on the device functioning as an electromechanical converter. The main characteristic of this machine is to maintain speed proportional to the feeding frequency [12], hence the name it carries, as it does not have a slip speed like an asynchronous machine.

The power management of this machine is carried out by a three-phase inverter controlled by different control loops programmed in the real-time simulation platform Opal RT. LD Didactic devices were used for the mechanical control of the system. In addition, the three-phase inverter, responsible for power control, has a DC bus powered by a bidirectional Chroma source. The assembly of the three-phase converter includes current and voltage sensors that are read by the Opal RT real-time simulation platform.

The power and control part of this plant is functioning correctly. However, when attempting to integrate the electrical power part with the mechanical part, an electromagnetic interference problem arises due to the unification of the grounding systems of LD Didactic and the control ports of Opal RT. This is due to a potential difference in the grounds of these devices.

When creating an isolated three-phase network, the problem arises of not having synchronization with the three-phase network that supplies power to the laboratory, along with a difference in potential between their grounds. Due to this issue, when connecting the control module of the pendulum machine (LD Didactic) to send the speed signal and receive the mechanical torque signal, an electrical failure occurs, resulting in the blocking of devices connected to the laboratory's three-phase network and posing an electrical risk if left connected for an extended period. The described phenomenon occurred within the human reaction time to perceive the error and turn off the system to prevent an accident.

This article discusses the proposed solution for managing variables between both devices and creating a broader prototype for emulating different generation systems and machine control. The main idea is to transmit data through a simple communication system, in this case, a PWM (Pulse Width Modulation) was implemented using an optical fiber channel. Pulse Width Modulation is a technique used to encode information or control the

output of a power system. In this application, it is used for a simultaneous wireless transfer of information and energy using a laser [13].

Taking into account the main variables required, conditioning of the analog speed signal is performed, which originates from the mechanical part module. This signal is then read by an ADC (Analog-to-Digital Converter) on the Raspberry Pi Pico microcontroller. The microcontroller performs PWM and sends the signal through an optical fiber transmitter module. The transmitted signal is then read by a receiver module connected to the Opal RT, and the duty cycle is retrieved to manipulate the signal. Similarly, the mechanical torque signal is sent from the power control to the mechanical control.

Finally, this article will address two types of experiments on the platform to verify the operation of the communication board designed for this system. The first test conducted is to manipulate the synchronous machine as a motor and vary the torque to measure the power it supplies or demands. The second experiment involves requesting power from the synchronous machine, which will have a fixed speed imposed by the pendulum machine to emulate the behavior of a wind generation system.

Furthermore, it is expected that with this type of platform, different control strategies and manipulation of converters focused on renewable energy can be tested, as seen in various articles published in the cloud. For example, in the article [14], it may transition from emulating the synchronous machine to directly working with one. Similarly, in the article [15], different control strategies for the conversion of wind energy to electrical energy using the back-to-back configuration are discussed. These platforms provide opportunities for experimentation and implementation of innovative control techniques in the field of renewable energy.

The development of the experimental platform to emulate wind turbines involved the implementation of a series of steps and techniques to integrate electrical and mechanical components. These steps included selecting and configuring appropriate devices, programming specific controllers, interconnecting components, resolving electromagnetic interference, implementing communication through PWM with optical fiber, and validating the controllers through testing. This methodology overcame technical challenges and successfully emulated wind turbines. It also lays the foundation for experimentation in control strategies and converter manipulation in the context of renewable energies, and for replicating this type of platforms.

2. General structure of a wind turbine

Current wind turbines essentially consist of two parts: a mechanical part and an electrical part. The first subsystem extracts wind energy and converts it into kinetic energy on a rotating shaft, while the second subsystem transforms that electrical energy to make it suitable for the power grid. Both subsystems are connected through an electric generator that converts mechanical energy into electrical energy [16].

The electrical part of the system is the back-to-back converter configuration. These converters can be seen as an extension of the electric generator in a wind turbine. They convert the electrical energy produced by the wind turbine into a form that can be easily exchanged with the main grid. This allows wind turbines to be connected to the main grid and contribute to the overall power supply. This platform generally has a back-to-back configuration, as shown in Figure 1. This configuration enables bidirectional energy exchange between the microgrid and the main grid, and it is used to isolate the microgrid from the main grid [17].

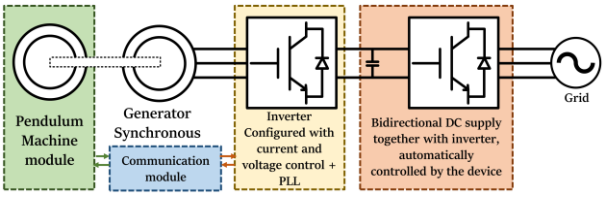

Figure 1: Representation of the back-to-back system connected to the synchronous machine (General Prototype).

In the first presented figure, two main power converters can be observed in the configuration, where the first inverter (from left to right) is capable of regulating the power flow from the generator, and the second inverter is responsible for regulating the DC bus, synchronizing with the power grid, and enabling bidirectional power flow between the system and the power grid.

In this experimental platform, we will be working with a synchronous machine that has a wide operating range, and with this system, we can observe its qualities and shortcomings when manipulated in four quadrants.

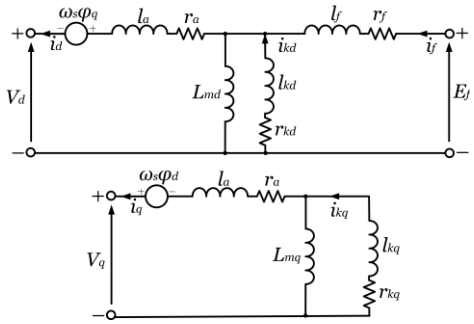

Figure 2: Equivalent circuit of the synchronous machine for dq reference.

The synchronous machine is a rotating electrical machine that converts mechanical power into electrical power or vice versa. It is a key component It is a key component in this paper, and its operation is governed by a set of equations. The equations of the synchronous machine can be divided into two groups: the d-axis equations and the q-axis equations. The d-axis equations describe the dynamics of the armature current and field current in the d-axis, while the q-axis equations describe the dynamics of the armature current and field current in the q-axis. [18]

The d-axis and q-axis equations are coupled by the mutual inductance between the d-axis and q-axis windings. The equations are also coupled by the damper windings, which are used to stabilize the machine's operation (This can be complemented with the equivalent circuit of the machine in the dq domain, presented in Figure 2). The equations of the synchronous machine are nonlinear and can be difficult to solve analytically. However, they can be solved numerically using computer simulations. The equations of the synchronous machine are an important tool for understanding the operation of the machine and for designing and controlling synchronous machines.

3. Experimental platform

The left inverter represented in Figure 1 is connected to a synchronous machine, which is mechanically coupled to a pendulum machine capable of establishing a fixed torque or a fixed speed depending on the test being conducted.

The left inverter was implemented with Semikron hardware, which consists of three branches of two IGBTs along with a branch for the DC bus, complying with the topology of a three-phase six-pulse inverter. It has respective current and voltage sensors for each phase and is controlled by the Opal RT. The inverter has a power of 10 kW. Further explanation of the control of this device will be provided in Section 3.2.

Regarding the right inverter in the diagram shown in Figure 1, the connection to the power grid is implicit in the operation of the bidirectional Chroma source. This source acts both as a load and a generator and is responsible for power injection into the grid. The referenced article [19] addresses the theory and management of this power injection, as well as the different controls of the converters. These controls, similar to those presented later in this article, are specifically designed for their application in the conventional grid. The stabilizing effects of frequency and voltage control loops in islanded and grid-connected operation scenarios are explored, along with stability requirements and inverter control adjustment strategies based on different types of loads, which the equipment used autonomously handles.

This bidirectional DC power supply can be used to supply or absorb power from the grid. It is ideal for a variety of applications, including, AC to DC power conversion, this can be used to charge batteries, power electronic devices, or perform laboratory tests. Absorption of power from renewable energy sources: This can be used to feed power back into the grid (objective of this paper) or to balance the load on a battery system and regulation of the DC bus of the back-to-back configuration. This source is capable of handling a power of 18 kW, which is more than sufficient for this 300 W generation application.

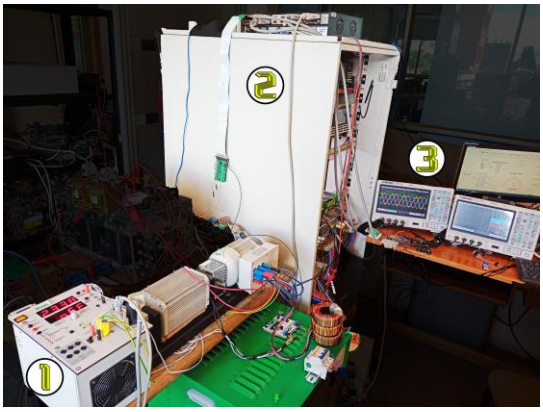

Figure 3: Photograph of the prototype implemented in the microgrid laboratory.

In Figure 3, three items are observed:

1. Reference is made to the mechanical part of the system, which will be addressed in more detail in section 3.2.
2. Shelf where the sensory part of the system is located, including the inverter, bidirectional

power source, control signal decoupling, and additional power sources required by the system.
3. System monitoring center.

3.1. Mechanical Section

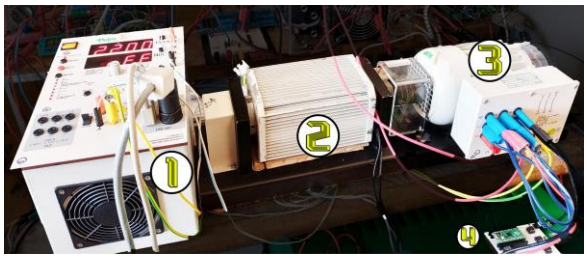

Figure 4: Specific photograph of the mechanical system, representation No. 1 of Figure 2*3.

In Figure 4, the hardware used in the mechanical system is shown, which consists of the following components:

1. Pendulum machine control module.
2. Pendulum machine.
3. Synchronous machine.
4. Communication module.

The control module is powered by a two-phase source of 220 V, with the speed variable as the output and the mechanical torque imposed by the pendulum machine as the input. Therefore, it is necessary to create a communication module, which will be explained in the following section. Within this module, there are different types of protections, such as temperature protection for the machine and a bidirectional power flow control. This control involves the torque-speed relationship at any given moment, which protects the power supply of the synchronous machine if it only operates as a source and not as a load. In the case of the experimental platform, it is prepared to work in all four quadrants. However, this protection needs to be deactivated from the module's startup in order to do so.

The synchronous machine being studied in this article has a rated power of 0.3 kW from the same company as the control module of the pendulum machine. The parameters of this machine are developed in another article [20], from which the armature resistance and field resistance: $R_a = 41.647\ \Omega, \mathrm{R_f} = 223.77\ \Omega$. The field and armature resistances can be calculated using the volt-ampere method, which consists of applying a series of different voltages to the synchronous machine and measuring the current that flows through it. The resistance is calculated by dividing the voltage by the current. Five attempts are performed for each resistance around the rated current. The values of Ra and Rf are used in the mathematical models of the machines (mentioned at the end of section 2) to calculate their dynamic behavior.

The linear magnetizing inductance, denoted as Lm, is expressed as

$$L_m = K_l/\omega_s \tag{11}$$

Where $K_l \approx 1260\ \frac{H}{rad/s}$, $L_m = 4.01\ H$. They also have the machine losses, and with these, they calculate the relative core loss resistance using the equation:

$$R_c = \frac{U_0^2}{P_{core}} \tag{12}$$

Given: $P_{mec} = 16.95W, U_0 = 400V,$
$P_{core} \approx 17.51W, \quad Rc \approx 9.14\ k\Omega.$

In addition, the article [20] describes other important parameters such as the synchronous reactances of the d-axis and q-axis.

3.2. Three-phase Inverter

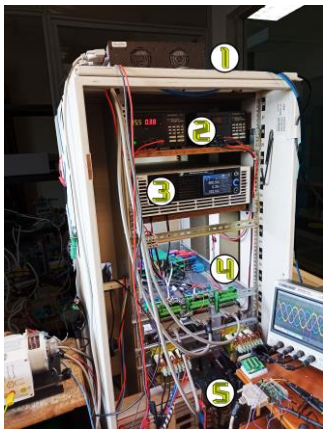

Figure 5: Specific photograph of the power system, representing No. 2 of Figure 2*3.

In the Figure 5, the following components of the power system are shown:

1. Opal RT: A device used for real-time control and simulation.
2. DC power supply: Used to bias the optocouplers of the inverter.
3. Bidirectional power supply: Provides DC power to the bus and is synchronized with the electrical grid.
4. System sensors and galvanic decoupling of control signals: Used for acquiring system

information and electrically isolating control signals.

5. Inverters and LC output filter: The inverter is connected to the synchronous machine and acts as a bidirectional converter. The LC filter is used to improve the quality of the output signal.

Regarding the inverter, it operates with pulse width modulation (PWM) generated by comparing a set of three-phase sinusoidal signals. This technique allows for control of the generation of the six pulses used in the inverter. A control model based on this modulation is developed.

The sensors located at the output of the inverter are used to perform the dq transformation, which is a mathematical transformation to work in an appropriate reference frame and perform the necessary controls. In the described case, current and voltage controls are implemented, as shown in Figure 6.

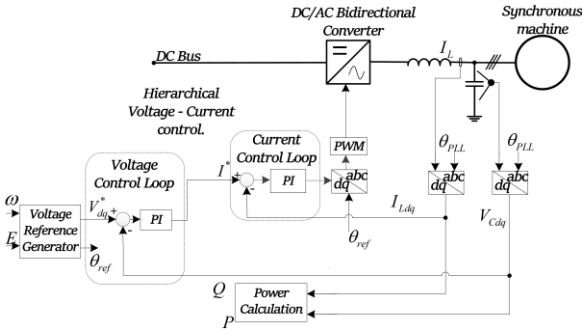

Figure 6: Block diagram representation of the hierarchical control of the inverter, voltage-current.

Regardless of the operating mode of the inverter, synchronization is programmed using a Phase-Locked Loop (PLL). The PLL is a widely used control system in electrical and electronic engineering. Its main function is to generate an output signal that is synchronized in phase and frequency with a reference input signal, in a mathematical way, the operation of the PLL is described in the block diagram presented in Figure 7. The PLL is employed in various applications, such as communication systems, control systems, among others. In power controllers with current control, the PLL is used to accurately extract the phase of the grid voltages [21] or in this case, the power of the synchronous machine.

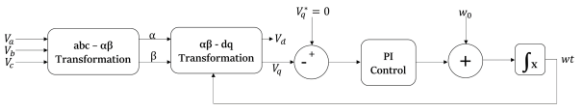

Figure 7: Block diagram representation of the Phase-Locked Loop (PLL).

There is a operating mode where the inverter operates solely as a current controller to control the active power flow delivered or received by the synchronous machine, as seen in Figure 8. In this case, the use of the PLL is necessary for the inverter to synchronize with the machine and perform the control.

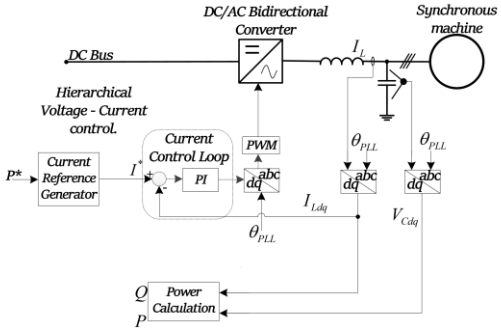

Figure 8: Block diagram representation of the current control of the inverter for active power extraction from the synchronous machine.

3.3. Optical communication

Figure 9 depicts a block diagram showing the components involved in optical communication. The blue arrows represent the channels of the optical fiber. Additionally, there are two predominant colors in the system: gray and orange. The gray color indicates that the blocks are connected to the ground of the mechanical module, while the orange color indicates that they are connected to the ground of the power control module.

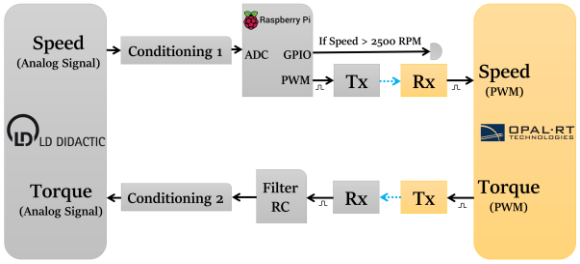

Figure 9: Representation of the systems involved in the designed optical communication.

This communication board was developed using the Raspberry Pi Pico microcontroller, which utilizes the RP2040 chip. Following the signal flow depicted in Figure 9, an analog signal needs to be conditioned before it can be sent to the microcontroller's analog-to-digital converter (ADC). The ADC employed is a Successive Approximation Register (SAR) ADC, which is designed to convert an analog signal into its digital equivalent. It utilizes the binary search algorithm to determine the

digital representation of the input signal. The SAR ADC consists of three main components: a digital-to-analog converter (DAC) that generates a comparison voltage, a SAR logic that configures the DAC, and a comparator that performs the comparison. During the conversion process, a sampling phase is conducted to capture the input signal, followed by a conversion phase where multiple comparisons are made to determine the digital bits. [22].

Once the internal reading is performed by this microcontroller, a PWM is applied to the data. Pulse Width Modulation (PWM) is a technique used in digital data transmission. It involves varying the duration of pulses in a digital signal to represent information. In the case of PWM generation, a modulating input signal and a sawtooth waveform are used for comparison to obtain a PWM output signal. The width of the pulses in the PWM signal represents the digital data to be transmitted. This technique is commonly used for transmitting digital data in communication systems, such as audio signal transmission or digital device control. [23].

However, other types of modulation such as PAM (Pulse Amplitude Modulation) or PPM (Pulse Position Modulation) can also be used. PAM modulates the amplitude of the pulses in a signal, while PPM modulates the temporal position of the pulses. Both types of modulation have specific characteristics and applications in signal transmission [24] [25].

The aforementioned aims to send the speed signal from the pendulum machine module to the Opal RT. Once the signal has been modulated into PWM, it is transmitted through optical fiber. This technology has the advantage of avoiding electrical problems and failures that were described at the beginning of this article. The optical fiber receiver is connected to the Opal RT, which is capable of detecting the frequency and instantaneous duty cycle of the signal. Using the duty cycle, the characteristic equation of the speed as a function of the duty cycle is obtained.

Similarly, the mechanical torque signal is sent from the Opal RT as a digital signal. Upon receiving it on the communication board through the optical fiber receiver, it is converted into an analog signal using an RC filter to be sent to the control module within the specific range of the pendulum machine. This prevents exceeding the machine's torque and avoiding potential failures.

Additionally, the module is equipped with a Wi-Fi device that allows sending the speed signal to an Internet database for future IoT applications of the prototype. A buzzer is also included on the board, indicating when the mechanical system is in an overload state, providing additional control over the system. This communication module can be seen in Figure 10.

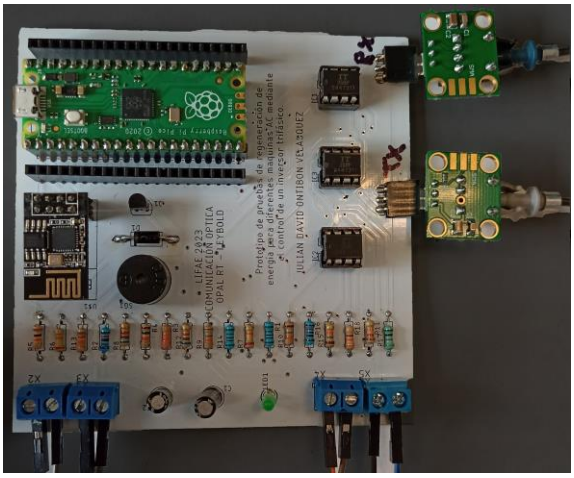

Figure 10: Specific photograph of the communication board designed for this emulation system.

4. Test and results

Once the prototype is completed, the first step is to verify the controls in the inverter and ensure that the DC power supply is functioning correctly. This can be observed in Figure 11, which shows the generation of a three-phase signal along with its triangular reference signal. In this case, a frequency of 60 Hz was used.

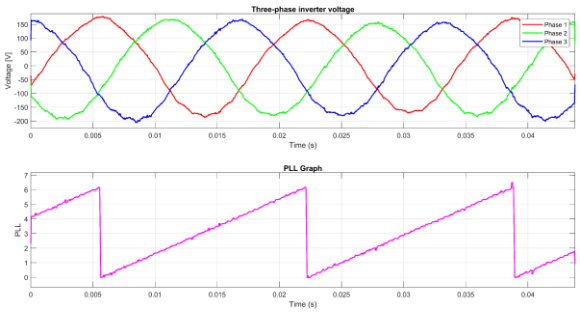

Figure 11: Three-phase output voltage of the inverter along with the triangular reference signal.

The first experiment aimed to use the machine as both a motor and generator simultaneously, with a varying torque during the test.

In the second experiment, a constant speed was imposed on the synchronous machine to operate it solely as a generator. In this case, current control was implemented to extract power.

The purpose of the first experiment was to explore the behavior of the machine when operating as both a motor and generator at the same time. The applied torque was varied during the test to observe its impact on performance and electrical characteristics. This variation allowed for valuable data collection on the machine's response under different load conditions.

In the second experiment, a constant speed was set for the synchronous machine. This specific configuration enabled the device to operate exclusively as a generator. Additionally, current control was applied to optimize power extraction from the machine.

The focus of the second experiment was to understand how the synchronous machine could generate stable and consistent current at a constant speed, and how current control could affect the device's power extraction capability. The results obtained provided valuable insights into the efficiency and performance of the synchronous machine under these specific operating conditions.

In summary, these two experiments allowed for the analysis and evaluation of various aspects of the machine's behavior, both in its motor-generator function and its ability to generate stable current and extract power in a controlled manner. The findings contribute to the advancement and understanding of the characteristics and applications of this specific platform.

4.1. Two-Quadrant Testing of the Synchronous Machine

In this section, the results and analysis of the test conducted on the synchronous machine operating in two quadrants (moving the requested torque from negative to positive values, transitioning from generator to motor, with the machine previously started) are presented. To facilitate the understanding of the collected data, various graphs have been generated illustrating the output signals from the Opal RT and the DC bus, as well as the active and reactive powers at the output of the inverter.

Figure 12 shows the Opal RT output signals in four quadrants. Quadrant I shows the requested torque, which ranges from -1 Nm to 1 Nm. Quadrant II shows the machine speed, which was fixed at 1800 RPM for this test. Quadrant III shows the active power output from the inverter, which shows the machine mode change (from generator to motor) from -300 W to 450 W. Quadrant IV shows the reactive power output from the inverter, which depends on the absolute magnitude of the torque. This is why it exhibits second-order behavior. These signals provide an integral view of the machine's behavior during the test. They allow the analysis of its performance under different conditions.

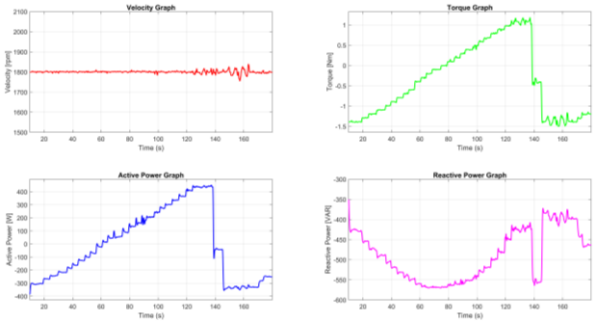

Figure 12: Output signals from the Opal RT. Requested Torque (Quadrant I), Machine Speed (Quadrant II), Active Power at the output of the inverter (Quadrant III), Reactive Power at the output of the inverter (Quadrant IV).

In addition, Figure 13 provides captures of the DC bus signals, including voltage (which is regulated to 500 V for this test), current, and power. These signals depend on the torque applied to the shaft. The data are specifically for the first operating mode (voltage and current control). The bidirectional source provides these data with a relatively low sampling rate of 1 second. However, they provide us with the information needed to analyze the losses in the inverter.

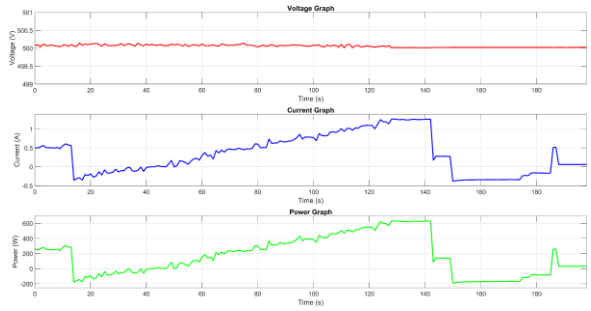

Figure 13: DC bus signals, captures by the bidirectional source, Voltage, Current, Power (For the first operating mode).

On the other hand, Figure 14 shows the power signals at both the DC bus and the three-phase point between the inverter and the machine. In addition, the requested torque is included in the graph. These signals are essential for understanding how the energy is distributed in different points of the system and evaluating the overall performance of the machine. The losses in the inverter for this voltage-current control mode are approximately 150 W. This is because the machine is operating in two quadrants and the voltage is controlled.

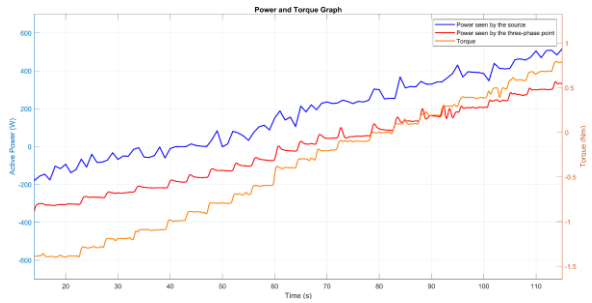

Figure 14: Power signals in the DC bus and three-phase point (Inverter-machine), along with requested torque.

In addition to the above, Figure 15 shows the active power graphs at the DC bus and three-phase point, as well as the reactive power as a function of mechanical torque. These graphs allow us to analyze the relationship between power and requested torque. They also allow us to check the losses between the input and output of the inverter, and to analyze the behavior of reactive power according to the torque.

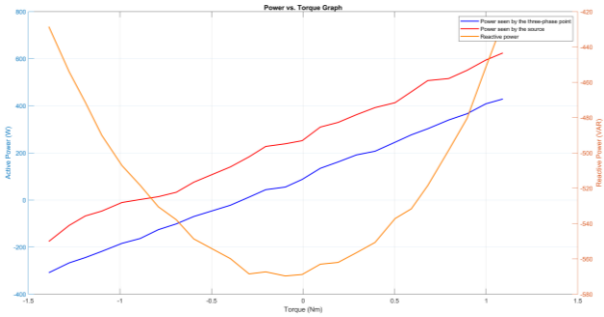

Figure 15: Active power graphs (DC bus and three-phase point) and reactive power as a function of mechanical torque.

The detailed analysis of the signals and results obtained in this two-quadrant test of the synchronous machine provides valuable information about its electrical behavior and power generation (Mechanical and electrical) capability under different operating conditions. These data enhance our understanding of the machine's characteristics and performance, laying the foundation for future studies and improvements in its operation.

4.2. Power control test on the synchronous generator.

In this section, we present the results and analysis of the power control test conducted on the synchronous generator. To facilitate the understanding of the obtained data, various graphs have been generated, illustrating the three-phase voltage generated by the synchronous machine, the synchronization provided by the PLL, the three-phase voltage of the inverter and generator operating at the same point, as well as the power delivered by the generator requested through the current control of the inverter.

Figure 16 shows the three-phase voltage generated by the synchronous machine at a speed of 1500 RPM, along with the synchronization graph provided by the PLL. These signals are fundamental to evaluate the quality and stability of the voltage generated by the machine, as well as its proper synchronization.

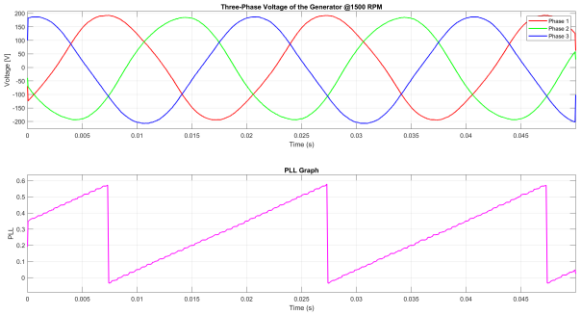

Figure 16: Three-phase voltage generated by the synchronous machine at a speed of 1500 RPM, along with the synchronization graph provided by the PLL.

On the other hand, Figure 17 presents the three-phase voltage of the inverter and generator operating at the same point. This graph allows evaluating the power control capability to maintain the voltage generated by the generator within the desired range and ensure proper synchronization.

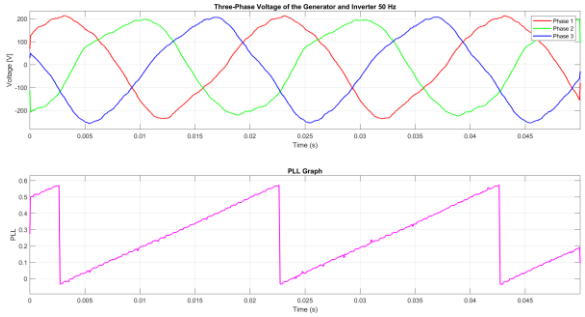

Figure 17: Three-phase voltage of the inverter and generator operating at the same point.

Figure 18 shows the graph of the power delivered by the generator, requested through the current control of the inverter. This signal reflects how the current control directly affects the power generated by the synchronous generator and allows us to evaluate the efficiency and precision of the control in energy extraction. It is observed that the control has an error of approximately 3%, which is clear in the case of the null power request

(0 W), where there is a small consumption of 10 W. This error is present in all the steps.

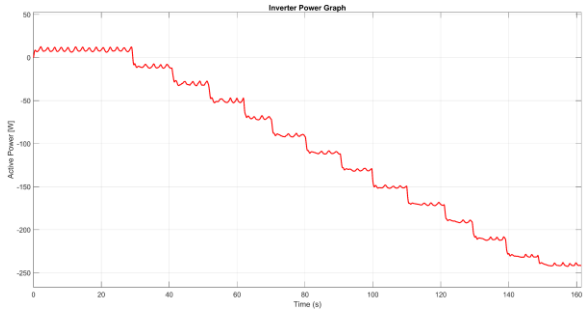

Figure 18: Graph of power delivered by the generator, requested through the current control of the inverter.

In addition, Figure 19 provides captures of the signals from the DC bus, including voltage, current, and power, specifically for the second setup. These data provide detailed information about the electrical behavior of the system in terms of power supply and flow in the DC bus.

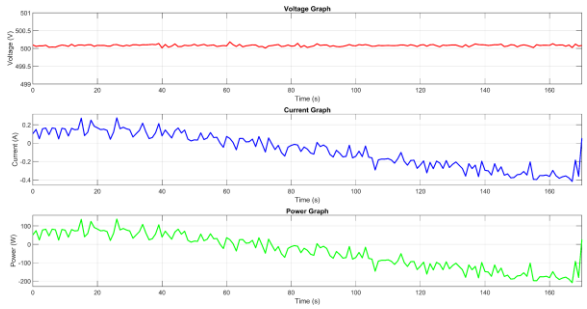

Figure 19: Signals from the DC bus, captured by the bidirectional source, Voltage, Current, Power (For this test).

Figure 20 shows the power signals at both the DC bus and the three-phase point between the inverter and the machine. These signals allow us to analyze how the energy is distributed in different points of the system and to evaluate the overall performance of the synchronous generator in terms of its generation and supply capacity. For the case of current control only, losses are observed between these two points of approximately 75 W. This is half the losses that are obtained when compared with the test that adds voltage control.

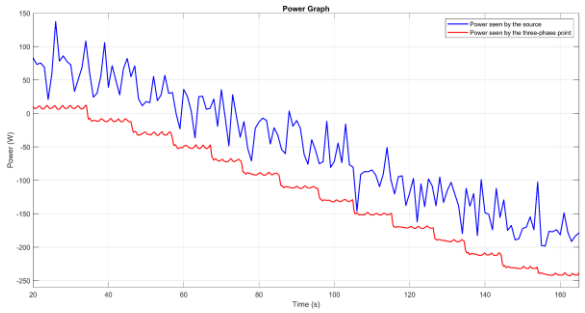

Figure 20: Power signals, at the DC bus and three-phase point (Inverter-machine).

Finally, Figure 21 presents the graphs of active power at the DC bus and at the three-phase point as a function of the requested power. These graphs allow analyzing the relationship between the requested power and the power delivered by the generator, providing essential information to evaluate the performance of the power control and its ability to meet power requirements.

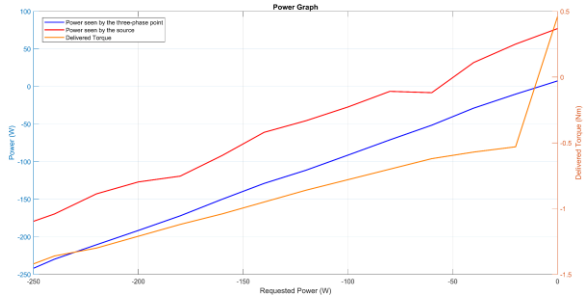

Figure 21: Graphs of Active Power (DC bus and Three-phase point) as a function of the requested power.

5. Conclusions

The experimental platform described in the article offers a working tool for the emulation of wind power systems using synchronous generators. The platform operates at a scale of 300 W, which limits it to academic use. This is due to the significant power losses in the three-phase inverter, which is 10 kW. These losses translate to a power loss of approximately 75 W. However, the platform works correctly as a tool for testing different controllers. In the case of current control for power extraction, there is an error of 3%, which is equivalent to approximately 10 W not extracted.

This platform provides the opportunity to conduct tests and experiments to test different control strategies in micro-grid-managed power generation systems. Future work is the implementation of a dynamic PLL and the application of different speed profiles on the pendulum machine. This will allow the analysis of power generation performance under different wind dynamics

in specific areas. The platform is capable of performing this type of task, as the work is handled in the models and not in the hardware.

Acknowlegment

This work was partially supported by Minciencias with the project *"Programa de Investigación en Tecnologías Emergentes para Microrredes Eléctricas Inteligentes con alta Penetración de Energías Renovables,"* contract number 80740-542-2020.

6. References

[1] R. Varon, Contextualización de la generación distrubuida de energía., Bogotá D.C.: EAN, 2020.

[2] Corficolombiana Investigaciones Económicas, "Perspectiva Sectorial Energía - Actualidad del Sector Energético Colombiano," Corficolombiana , Bogota D.C., 2023.

[3] Unidad de Planeación Minero Energética, "Proyección Demanda Energía Eléctrica y Combustibles Líquidos," UPME, Bogotá D.C., 2022.

[4] Cigre Colombia, "REGULACIÓN, NORMATIVA Y NUEVOS MERCADOS EN MICRORREDES EN EL SECTOR ELÉCTRICO COLOMBIANO," Comité de Estudios C5 Mercados de Electricidad y Regulación, Medellin, 2021.

[5] M. Uddin, H. Mo, D. Dong, S. Elsawah, J. Zhu and J. M. Guerrero, "Microgrids: A review, outstanding issues and future trends," *Energy Strategy Reviews,* vol. 49, no. 101127, pp. 101-127, 2023.

[6] S. B. A. Kashem, S. D. Souza, A. Iqbal and J. Ahmed, "Microgrid in Military Applications," in *IEEE 12th International Conference on Compatibility, Power Electronics and Power Engineering (CPE-POWERENG 2018)*, Doha, 2018.

[7] M. Waseem, M. A. Khan, A. Goudarzi, S. Fahad, I. A. Sajjad and P. Siano, "Incorporation of Blockchain Technology for Different Smart Grid Applications: Architecture, Prospects, and Challenges," *energies,* vol. 16, no. 2, p. 29, 2023.

[8] M. S. Sami, M. Abrar, R. Akram, M. M. Hussain, M. H. Nazir, M. S. Khan and S. Raza, "Energy Management of Microgrids for Smart Cities: A Review," *energies,* vol. 14, no. 18, p. 18, 2021.

[9] A. Padilla-Medina, F. Perez-Pinal, A. Jimenez-Garibay, A. Vazquez-Lopez and J. Martinez-Nolasco, "Design and Implementation of an Energy-Management System for a Grid-Connected Residential DC Microgrid," *energies,* vol. 13, no. 16, p. 30, 2020.

[10] M. H. Saeed, W. Fangzong, B. A. Kalwar and S. Iqbal, "A Review on Microgrids' Challenges & Perspectives," *IEEE Access* , vol. 9, no. 21408762, pp. 166502 - 166517, 2021.

[11] S. Ahmad, M. Shafiullah, C. B. Ahmed and M. Alowaifeer, "A Review of Microgrid Energy Management and Control Strategies," *IEEE Access,* vol. 11, no. 22759634, pp. 21729 - 21757, 2023.

[12] D. D. Calvo, Control de una máquina síncrona como motor paso a paso y generador, Valladolid: Universidad de Valladolid, 2019.

[13] Y. Wang, C. Zhao, L. Zhang, Z. Zhang and H. Zhang, "Hybrid pulse-widh-modulation-based simultaneous wireless laser information and power transfer system using PWM sampling," *Optics Commuunications,* vol. 515, no. 128232, pp. 1-6, 2022.

[14] M. ASHABANI and J. JUNG, "Synchronous Voltage Controllers: Voltage-Based Emulation of Synchronous Machines for the Integration of Renewable Energy Sources," *IEEE Acess,* vol. 8, pp. 49497 - 49508, 2020.

[15] H. Matayoshi, A. M. Howlader, M. Datta and T. Senjyu, "Control strategy of PMSG based wind energy conversion system under strong wind conditions," *Energy for Sustainable Development,* vol. 45, pp. 211-218, 2018.

[16] R. Teodorescum, M. Liserre and P. Rodríguez, GRID CONVERTERS FOR PHOTOVOLTAIC AND WIND POWER SYSTEMS, Aalborg: WILEY, 2011.

[17] R. Alayi, F. Zishan, M. Mohkam, S. Hoseinzadeh, S. Memon and D. A. Garcia, "A Sustainable Energy Distribution Configuration for Microgrids Integrated to the National Grid Using Back-to-Back Converters in a Renewable Power System," *Electronics MDPI,* vol. 10, no. 1826, pp. 1-21, 2021.

[18] M. Larakeb, A. Bentounsi and H.Djeghloud, "On-Line Parameters Estimation of Low Scale SPSG Using Discrete Kalman Filters," *Journal of Electrical Systems,* vol. 12, no. 4, pp. 770-785, 2016.

[19] Z. Zhou, W. Wang, D. Ramasubramanian, E. Farantatos and G. M. Huang, "Small Signal

Stability of Phase Locked Loop based Current-Controlled Inverter in 100% Inverter-based System," *IEEE Transactions on Sustainable Energy*, vol. 14, no. 3, pp. 1612 - 1623, 2023.

[20] H. Djeghloud, A. Bentounsi and M. Larakeb, "Real and Virtual Labs for Enhancing a SM Course," in *International Conference on Electrical Machines and Systems (ICEMS)*, Sapporo, 2012.

[21] S. Ahmad, S. Mekhilef and H. Mokhlis, "An improved power control strategy for grid-connected hybrid microgrid without park transformation and phase-locked loop system," *International Transactions On Electrical Energy Systems*, vol. 31, no. 7, pp. 1-32, 2021.

[22] X. Tang, J. Liu, Y. Shen, S. Li, L. Shen, A. Sanya, K. Ragab and N. Sun, "Low-Power SAR ADC Design: Overview and Survey of State-of-the-Art Techniques," *IEEE Transactions on Circuits and Systems I: Regular Papers*, vol. 69, no. 6, pp. 2249 - 2262, 2022.

[23] A. Shankar, A. Lokeshwari, B. Manohar and S. Pranavi, "IMPLEMENTATION OF SIMPLE PWM/PPM GENERATOR FOR MICROCONTROLLER USING VERILOG," *International Journal of Advanced Research in Engineering and Technology (IJARET)*, vol. 12, no. 3, pp. 97-102, 2021.

[24] Hossien, M. Eftiaz, Zahir, M. Z. Ibne and S. M. R. Karim, "Performance Analysis of PAM and PPM in Communication System," *International Journal of Scientific & Engineering Research*, vol. 10, no. 7, pp. 752-757, 2019.

[25] H. HAMIL, M. S. AZZAZ, S. SAKHI, A. MAALI, Z. Zidelmal and D. O. Abdeslam, "Design and FPGA real-time implementation of PWM and PPM modulation for Ultra Wide Band applications," in *International Conference on Image and Signal Processing and their Applications (ISPA)*, Mostaganem, 2019.